Peripheral cannulae selection for veno-arterial extracorporeal life support: a paradox

Yuri M Ganushchak,[*,1] **Eva R Kurniawati,**[*,1] (iD) **Jos G Maessen**[1,2] **and Patrick W Weerwind**[1,2]

Abstract

Explosive penetration of veno-arterial extracorporeal life support in everyday practice has drawn awareness to complications of peripheral cannulation, resulting in recommendations to use smaller size cannulae. However, using smaller cannulae may limit the effectiveness of extracorporeal support and thereby the specific needs of the patient. Selection of proper size cannulae may therefore pose a dilemma, especially since pressure-flow characteristics at different hematocrits are lacking. This study evaluates the precision of cannula pressure drop prediction with increase of fluid viscosity from water flow-pressure charts by M-number, dynamic similarity law, and via fitted parabolic equation. Thirteen commercially available peripheral cannulae were used in this in vitro study. Pressure drop and flow were recorded using water and a water-glycerol solution as a surrogate for blood, at ambient temperature. Subsequently, pressure-flow curves were modeled with increased fluid viscosity ($0.0031 \text{ N s m}^{-2}$), and then compared by M-number, dynamic similarity law, and fitted parabolic equation. The agreement of predicted and measured values were significantly higher when the M-number (concordance correlation = 0.948), and the dynamic similarity law method (concordance correlation = 0.947) was used in comparison to the fitted parabolic equation (concordance correlation = 0.898, p < 0.01). The M-number and dynamic similarity based model allow for reliable prediction of peripheral cannula pressure drop with changes of fluid viscosity and could therefore aid in well-thought-out selection of cannulae for extracorporeal life support.

Introduction

Veno-arterial extracorporeal life support (ECLS) is an *ultima ratio* therapy for cardiac failure. The ECLS results in stabilization of hemodynamics and resolving lactic acidosis, giving time for recovery of cardiac function. Veno-arterial ECLS saves one-third of patients unresponsive to any other resuscitative treatment after adult cardiac surgery as well as after refractory cardiac arrest.[1–4]

Most often ECLS requires access to peripheral vessels using suitable venous and arterial cannulae that permit an optimal flow rate typically above $2.0–2.3 \text{ L min}^{-1}\text{m}^{-2}$ [5] or even up to $2.5 \text{ L m}^{-2} \text{min}^{-1}$.[6,7] Adequate circulation sustained by extracorporeal support is necessary for effective and fast lactate clearance, as high rate of lactate clearance during the first hours of ECLS has been associated with decreased mortality.[8,9] Conversely, failure to clear lactate may worsen the outcome.

Explosive penetration of ECLS therapy in everyday intensive care unit practice has drawn awareness to complications of peripheral cannulation.[10] The incidence of both early and late vascular complications ranges from 10% to 70%.[11,12] To avoid such complications, it is recommended to use smaller cannulae as previous studies claimed that a 15Fr arterial cannula appears to provide adequate hemodynamic support.[13–16] However, this statement is based on a relatively small

[1]Department of Cardiothoracic Surgery, Maastricht University Medical Center+, Maastricht, The Netherlands
[2]Cardiovascular Research Institute Maastricht, Maastricht University Medical Center+, Maastricht, The Netherlands

*Yuri M Ganushchak and Eva R Kurniawati have contributed equally to this study.

Corresponding author:
Eva R Kurniawati, Department of Cardiothoracic Surgery, Maastricht University Medical Center+, P. Debyelaan 25, PO Box 5800, 6202 AZ Maastricht, The Netherlands.
Email: eva.kurniawati@mumc.nl

Table 1. Geometrical characteristics of cannulas.

Cannula	Length[a] (m)	M-number[b]		D$_e$ (mm)	Q (L min^{-1})	
		Avg.	Std		Re = 2,300 [f]	Re = 4,200 [ff]
Biomedicus 8Fr	0.19	4.41	0.01	2.19	0.68	1.24
Biomedicus 10Fr	0.19	3.93	0.01	2.77	0.86	1.56
Biomedicus 15Fr	0.4	3.30	0.01	4.39	1.36	2.48
Biomedicus 17Fr	0.4	3.03	0.02	5.00	1.55	2.82
Biomedicus 19Fr	0.4	2.83	0.01	5.52	1.71	3.12
EOPA 20Fr	0.28	2.76	0.01	5.30	1.64	2.99
EOPA 22Fr	0.28	2.52	0.01	5.96	1.84	3.36
EOPA 24Fr	0.28	2.45	0.01	6.15	1.90	3.47
Maquet 21Fr	0.34	2.68	0.01	5.73	1.77	3.23
Maquet 23Fr	0.75	2.60	0.01	7.04	2.18	3.97
Avalon 24Fr	0.8	2.47	0.01	7.58	2.34	4.28
Biomedicus 21Fr	0.8	2.83	0.01	6.38	1.97	3.60
Biomedicus 25Fr	0.8	2.48	0.01	7.56	2.34	4.27

D$_e$: cannula effective diameter; [f] flow below is laminar (viscosity of 0.0031 N s m^{-2}); [ff] flow above is developed turbulent (viscosity of 0.0031 N s m^{-2}).
[a]Distance from the tip of cannula to the pressure sensor.
[b]M-number between 50 and 100 mmHg pressure drop.

sample size and therefore it is difficult for a justified interpretation.[6] In practice, the lack of experience during peripheral cannulation is the trigger of many complications,[17] and after only a short learning curve, femoral cannulation has a lower complication risk.[18,19]

Commonly, the French scale (Fr) is used in the medical catheter industry. This scale describes only the catheter's outer diameter.[20] Some information can be acquired from the flow-pressure curves presented in the instructions for use. Nevertheless, these flow-pressure curves are based on tests performed with water at room temperature. The prediction of flow through a complex cannula shape can be described analytically by using computational fluid dynamics models.[21] This method is particularly useful when trying to evaluate flow in a setting with bends, drainage holes, and variable cross-sections. Computer simulations can be difficult as high spatial and temporal resolution are needed for accurate results.[21] There are several simpler methods to estimate the changes in flow-pressure relationship with changing of fluid viscosity. One is similar to the concept of impedance using the geometrical component (M-number),[22,23] and two other methods are based on the concept of dynamic similarity.[24–27]

The aim of this study was to evaluate the precision of flow-pressure relationship prediction from water flow-pressure charts by M-number, dynamic similarity law, and via fitted parabolic equation.

Materials and methods

Thirteen commercially available arterial and venous cannulae (Table 1) for peripheral cannulation were included in this study. Measurements were performed in
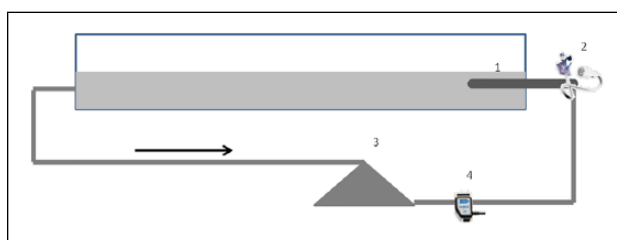
Figure 1. Flow pressure relationship measurement set-up. 1: cannula; 2: pressure sensor; 3: centrifugal pump; 4: flow probe. The direction of flow depends on the type (arterial or venous) of tested cannula.

a mock circulation (Figure 1) that consisted of a container with 10 L volume and a centrifugal pump (Rotaflow, Maquet Cardiopulmonary, Rastatt, Germany). A calibrated flow meter (Transonic Systems Inc., Ithaca, USA) was used for flow recording. The concerned cannula was introduced under the fluid level (± 1–2 cm) and was placed as far as possible from the distal wall of the reservoir to decrease the potential influence of rotational flow movement. Subsequently, the flow rate was slowly increased from 0 L min^{-1} to a maximal allowable flow rate and then back to 0 L min^{-1}. Each measurement was repeated three times. Flow and pressure were recorded using a custom-built data acquisition system (M-PAQ, Instrument Development Engineering & Evaluation, Maastricht University Medical Center, Maastricht, the Netherlands), and recorded first with water as a pumping fluid at a room temperature of 22°C. The second set of tests was performed using a water-glycerol solution with a viscosity of 0.0031 N s m^{-2}. The necessary mass concentration of glycerol was computed as described by

N-S Cheng.[28] The chosen viscosity of 0.0031 N s m^{-2} matches the viscosity of blood with a hematocrit of 30%.[29,30] Each set of flow pressure recordings for each cannula was categorized by creation of 51 ordinal levels by flow.

The flow pressure curves recorded with water as a pumping fluid were used to predict the pressure drops with increasing of viscosity (0.0031 N s m^{-2}). The first method for predicting pressure drop was based on the geometrical characteristic of a cannula, and presented as the M-number.[22] The M-number is a logarithm function of the geometric constant of the cannula and was computed from the flow-pressure data of the water tests using equations (1)-(3)

$$LD_e^{-(5+m)} = \left(2^m \times \pi^{(2+m)} \times 8^{-(1+m)} \times C^{-1} \right) \left(\mu^m \times \rho^{-(1+m)} \right) \times \Delta P \times Q^{-(2+m)} \quad (1)$$

where L is the total length of cannula (cm), D_e is the effective (hydraulic) diameter (cm), μ is the fluid viscosity (poise), ρ is the fluid density (g cm^{-3}), ΔP is the pressure drop through the cannula (dyn cm^{-2}), and Q is the flow (mL s^{-1}).

The constants C and m depend upon flow regimes.[31] Substitution of C = 0.316 and m = −0.25 into formula 1 results in

$$LD_e^{-4.75} = 7.161e6 \times \mu^{-0.25} \times \rho^{-0.75} \times \Delta P \times Q^{-1.75} \quad (2)$$

where ΔP is the pressure drop through the cannula (mmHg), and Q is the flow (mL min^{-1})

$$M = Log_{10} \left(LD_e^{-4.75} \right) \quad (3)$$

The other two methods are based at the concept of dynamic similarity.[24–27] In fluid mechanics, the dynamic similarity phenomenon states that in two geometrically similar vessels, (same shape but different sizes) flows are becoming identical if the Reynolds number (Re) is identical for both fluids.[27] The flow-pressure relationship can be transformed to those at different viscosity and density of flowing fluid according to equations (4) and (5)[25,27]

$$Q_b = Q_w \times v_b \times v_w^{-1} \quad (4)$$

$$P_b = P_w \times \rho_b \times \rho_w^{-1} \times \mu_b^2 \times \mu_w^{-2} \quad (5)$$

where b is the *blood (water-glycerol solution)*, w is the *fluid (water)*, Q is the flow (m^3 s^{-1}), P is the pressure (Pa), μ is the dynamic viscosity (N s m^{-2}), v is the *kinematic viscosity* (m^2 s^{-1}), and ρ is the density (kg m^{-3})

The third method requires mathematical function that has the best fit to flow-pressure data points. In this case, this is a fitted parabolic equation[25,27] (equation (6)). The coefficients "a" and "b" are rescaled by equations (7) and (8). The pressure drop can be predicted by equation (9)

$$\Delta P_w = a_w \times Q_w^2 + b_w \times Q_w \quad (6)$$

$$a_b = a_w \times \rho_b \times \rho_w^{-1} \quad (7)$$

$$b_b = b_w \times \mu_b \times \mu_w^{-1} \quad (8)$$

$$\Delta P_b = a_b \times Q_w^2 + b_b \times Q_w \quad (9)$$

where b is the *blood (water-glycerol solution),* w is the *fluid (water)*, Q is the flow (m^3 s^{-1}), P is the pressure (Pa), μ is the dynamic viscosity (N s m^{-2}), and ρ is the density (kg m^{-3}).

The values of flow and pressure of each category were used for computing the intraclass correlation (ICC) and concordance correlation (CCC) as measures of agreement between measured and derived flow-pressure curves. These correlation methods are described elsewhere.[32–35] The effective (hydraulic) diameter and Re were determined for each cannula (equations (10) and (11))

$$D_e = \left(L \times 10^{-M} \right)^{(1/4.75)} \quad (10)$$

where D_e is the effective (hydraulic) diameter of cannula (m), L is the length of cannula (m), and M is the geometric constant of cannula

$$Re = 4 \times \rho \times Q \times \left(\mu \times \pi \times D_e \right)^{-1} \quad (11)$$

where ρ is the density (kg m^{-3}), Q is the flow (m^3 s^{-1}), μ is the dynamic viscosity (N s m^{-2}), and D_e is the effective (hydraulic) diameter of cannula (m).

Excel 2010 with VBA and SPSS 23 were used for preparation and statistical data analysis, respectively. A p value less than 0.05 was recognized as statistically significant.

Results

The list of cannulae evaluated for this study is presented in Table 1. The length in meters is the actual distance between the cannula tip and pressure sensor, and D_e is the effective (hydraulic) diameter of the cannula derived from the M-number. The M-number calculation from the measured flow and pressure slowly increased with an
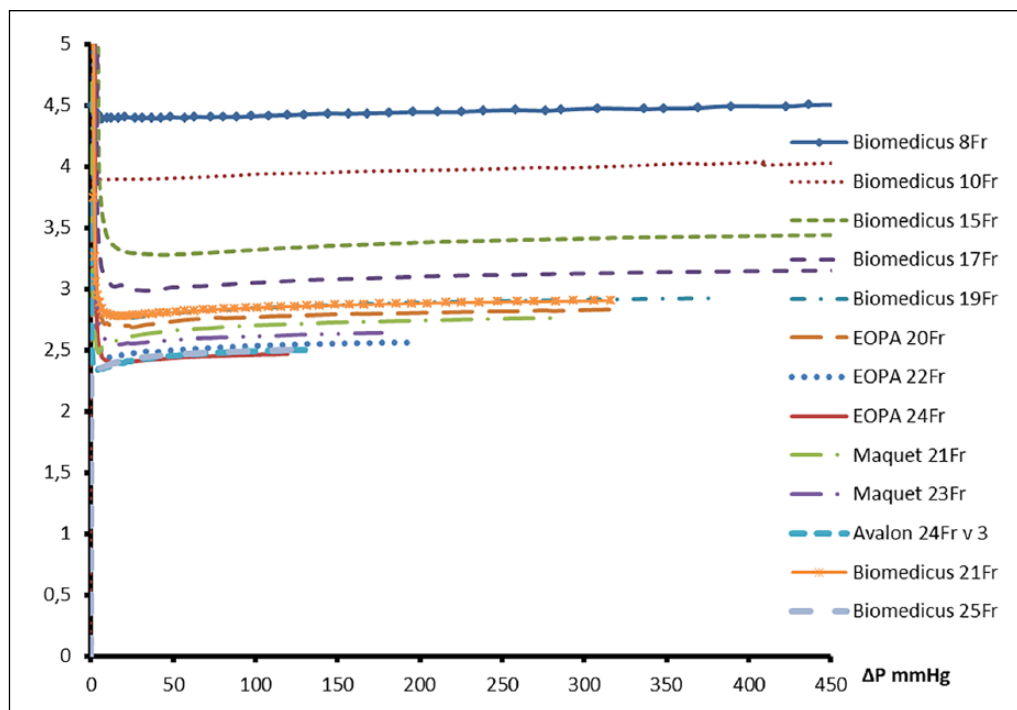
Figure 2. M-number of cannulae in the study against the pressure gradient due to water flow. M-number of all cannulae demonstrated slow *incensement* with rise of pressure gradient.

elevated pressure drop (Figure 2). The changes of the M-number with increase of pressure drop from 50 to 100 mmHg did not exceed ±1.5%. There was a high agreement between M-number computed from the water test results and tests with a water-glycerol solution. The M-number change with pressure drops for a Biomedicus 19Fr femoral arterial cannula, for example, is presented in Figure 3 (ICC = 0.977, p < 0.001). The average values of the M-number in the range of a pressure drop between 50 and 100 mmHg are presented in Table 1. These M-number values were used in the calculation of the effective (hydraulic) diameter for each cannula.

Flow-pressure models with a viscosity of 0.0031 N s m^{-2} were computed for all cannulae using three methods as previously described. Figure 3 depicts an example of measured and modeled pressure drop for the Biomedicus 19Fr femoral arterial cannula, using a water-glycerol solution with a viscosity of 0.0031184 Pa s. The agreement between the modeled and measured flow-pressure relation is shown in Table 2. All models showed a strong agreement with measured flow-pressure curves. However, the CCC coefficient of model-based at the parabolic regression was significantly lower (p < 0.01) in comparison to the M-number and the dynamic similarity based models (Table 2).

Noteworthy, all tested cannulae reached the transition Reynolds number (≈2,300) at flows less than 2.5 L min^{-1} (Table 1, water-glycerol solution with a viscosity of 0.0031 N s m^{-2}).
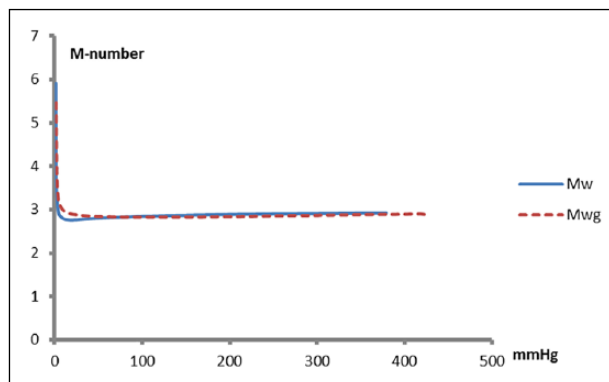
Figure 3. M-number of cannula against the pressure gradient. M_w: M-number computed from the flow-pressure data from water test; M_{wg}: M-number computed from the flow-pressure data from water-glycerol test (viscosity 0.0031184 Pa s), ICC = 0.977, p < 0.001; Biomedicus 19Fr femoral arterial cannula.

Discussion

Selection of the right cannulae based on the patient's body surface area and required support flow is important for the balance between providing adequate perfusion and minimizing damage to red blood cells.[6] In this study, the geometrical cannula component (M-number) showed to be precise and easily used for predicting pressure drop for the clinical relevant flow spectrum.

Table 2. Concordance and intraclass correlation coefficients for agreement measured and predicted flow-pressure curves.

	Model 1		Model 2		Model 3	
	CCC	ICC	CCC	ICC	CCC	ICC
Biomedicus 8Fr	0.911	0.983	0.962	0.993	0.722	0.948
Biomedicus 10Fr	0.982	0.997	0.994	0.983	0.879	0.999
Biomedicus 15Fr	0.683	0.914	0.562	0.923	0.787	0.907
Biomedicus 17Fr	0.997	0.999	0.983	0.991	0.934	0.997
Biomedicus 19Fr	0.990	0.996	0.994	0.997	0.939	0.989
EOPA 20Fr	0.983	0.995	0.990	0.995	0.938	0.988
EOPA 22Fr	0.967	0.993	0.985	0.993	0.934	0.987
EOPA 24Fr	0.991	0.997	0.951	0.994	0.981	0.940
Maquet 21Fr	0.975	0.991	0.983	0.995	0.912	0.982
Maquet 23Fr	0.980	0.997	0.981	0.995	0.951	0.993
Avalon 24Fr	0.940	0.990	0.965	0.995	0.878	0.982
Biomedicus 21Fr	0.978	0.995	0.992	0.996	0.924	0.986
Biomedicus 25Fr	0.945	0.992	0.971	0.998	0.900	0.986
Average	0.948	0.988	0.947	0.988	0.898*	0.976

CCC: concordance correlation; ICC: intraclass correlation.
Model 1: M-number based model; Model 2: dynamic similarity model; Model 3: parabolic equation model.
*$p < 0.01$ in comparison to Model 1 and Model 2.

Inserting a larger lumen cannula is more likely to cause local vascular trauma, downstream ischemia, or obstruction of venous return.[36] In addition, cannulae impact the system pressures, blood trauma as well as the pump flow rate during extracorporeal support.[37] These limitations can have devastating effects in case of ongoing cardiac function decline or during the necessity to increase the support flow. Furthermore, each specific cannula relates to a point where the flow becomes at first disturbed and then subsequently at increasing flow rates turbulent. This transition depends on many factors, such as wall roughness, fluctuations in the inlet stream, or presence of side holes, but primarily the Reynolds number. The transition Reynolds number for flow in a circular pipe is $Re_{crit} \approx 2,300$, where fully turbulent flow develops at $Re_d \approx 4,200$.[31] At these flow rates, local fluid velocities are unpredictable, but they are higher than the mean forward velocity.[38] Our data showed that the transition Reynolds number for the femoral arterial as well as venous cannulae reached flows less than 2.5 L min⁻¹. However, a fully turbulent flow via cannulae with an effective diameter of more than 6 mm was developed with flow rates above 4 L min⁻¹ (Table 1). These data are higher as suggested by Gordon Write[38] for cannulae with an effective diameter of 6–8 mm. A logical explanation for this difference lies in the fact that in our study, a viscosity of 0.0031 N s m⁻² was used. Although, the underlying mechanisms of turbulence-induced trauma are not clear, turbulent flow produces far more blood trauma than laminar flow under identical shear stresses.[39] In turn, haemolysis appears to be an important contributor to postoperative kidney injury and intestinal mucosal damage, caused potentially by limiting NO-bioavailability.[40,41] In addition, an improper-sized venous cannula entails increased subatmospheric venous line pressures and may cause direct damage to red cells[42] as well as *de-novo* gas emboli formation.[43–46] Existence of a narrow "allowable operating region" of magnetic driven centrifugal pumps[47,48] further emphasizes the importance of proper cannula selection. High line pressures and pump speeds shift the centrifugal pump characteristics to the left of the so-called "allowable operating region," resulting in recirculation, blood and impeller damage, low flow cavitation or even pump heating.[48,49]

Thus, proper selection of cannulae for ECLS is a careful balance between required flow, cannulation site, vessel diameter, and it has to be based on interdisciplinary knowledge. The challenge of cannulae selection is amplified by most common use of the French scale in the medical industry,[20] which is a uniform scale with even increments. Each increment of French sizing equals 0.33 mm. The disadvantage of the French scale is that it represents the outer diameter rather than the inner diameter of the catheter or tubing. It is clear that cannulae with the same outer diameter do not necessarily share the same performance characteristics.[23] Some information can be acquired from the flow-pressure curves presented in the industry's brochures. However, there is an important difference between the flow-pressure curves based on the tests with water and pressure gradients and with blood because of the large difference in the viscosity of blood and water.[36,37]

Translational research is essential to provide data, which can more accurately reflect the relation between pressure and flow of the cannula for clinical use.[36] The prediction of blood flow through complex shapes of cannulae can only be done with computational fluid dynamics models, which are complex and only possible using commercial packages.[21] There are several simplified methods, like the "M-number"[22,23] or methods based at the concept of dynamic similarity.[24–27] In this study, the agreement between measured flow-pressure curves and predicted pressure drop by three methods was compared (Table 2). Our data does not support the statement by De Somer[27] that the M-number cannot be used for prediction of pressure drop over a cannula. We demonstrated the independence of using the M-number for a viscosity-based pumping fluid (Figure 3). Moreover, the M-number was relatively stable at pressure drops of 50–100 mmHg (Figure 4). These findings confirm the theoretical conclusion that the M-number acts as the product of the geometrical component of a cannula.[22] The average CCC and ICC coefficients between measured and predicted values by the M-number and by the dynamic similarity law were significantly higher than predicted by the fitted parabolic equation. The method based on the dynamic
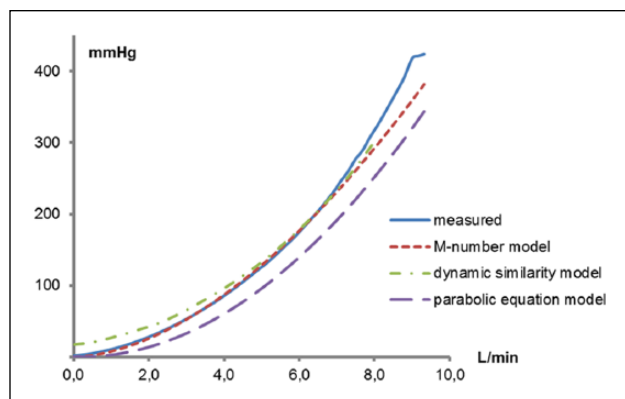
Figure 4. Example of pressure drop predictive models in comparison to the measured pressure. Biomedicus 19Fr femoral arterial cannula; water-glycerol solution viscosity 0.0031184 Pa s.

similarity, on the contrary, requires all digital flow-pressure data for computing flow and pressure drop with changes of pumping fluid. The M-number can be computed from a single pair of flow and pressure. The geometrical component of a cannula can therefore be easily used for predicting the pressure drops through the whole flow spectrum. Hence, we developed an Excel VBA application for modeling of pressure drop over a cannula (Supplemental Appendix 1).

Despite the described applicability of the M-number for precise prediction of pressure drops over cannulae, one has to be aware that flow-pressure charts as well as the model using the M-number give the minimum possible pressure drops in optimal conditions. In the clinical setting, the intravascular cannula position may affect the performance due to hypovolemia, or induced turbulence and secondary flows.[21,22] Another limiting factor when interpreting our results is the importance of the manufacturing tolerance range for cannulae, especially for smaller cannulae, as this might affect the calculations.[27]

In conclusion, the M-number allows for a reliable and easy prediction of pressure drops of cannulae with changes of fluid viscosity, and can therefore aid in a well-thought-out selection of cannulae for ECLS.

Declaration of Conflicting Interests

Funding

ORCID iD

Eva R Kurniawati https://orcid.org/0000-0002-8637-530X

References

1. Biancari F, Perrotti A, Dalen M, et al. Meta-analysis of the outcome after postcardiotomy venoarterial extracorporeal membrane oxygenation in adult patients. *J Cardiothorac Vasc Anesth* 2018; 32: 1175–1182.
2. Dennis M, McCanny P, D'Souza M, et al. Extracorporeal cardiopulmonary resuscitation for refractory cardiac arrest: a multicentre experience. *Int J Cardiol* 2017; 231: 131–136.
3. Demondion P, Fournel L, Golmard JL, et al. Predictors of 30-day mortality and outcome in cases of myocardial infarction with cardiogenic shock treated by extracorporeal life support. *Eur J Cardiothorac Surg* 2014; 45: 47–54.
4. Guenther S, Theiss HD, Fischer M, et al. Percutaneous extracorporeal life support for patients in therapy refractory cardiogenic shock: initial results of an interdisciplinary team. *Interact Cardiovasc Thorac Surg* 2014; 18: 283–291.
5. Extracorporeal Life Support Organization. ELSO general guidelines for all ECLS cases (version 1.4), www.elso.org (2017, accessed 22 October 2018).
6. Jayaraman AL, Cormican D, Shah P, et al. Cannulation strategies in adult veno-arterial and veno-venous extracorporeal membrane oxygenation: techniques, limitations, and special considerations. *Ann Card Anaesth* 2017; 20: S11–S18.
7. Pavlushkov E, Berman M, Valchanov K. Cannulation techniques for extracorporeal life support. *Ann Transl Med* 2017; 5: 70.
8. Li CL, Wang H, Jia M, et al. The early dynamic behavior of lactate is linked to mortality in postcardiotomy patients with extracorporeal membrane oxygenation support: a retrospective observational study. *J Thorac Cardiovasc Surg* 2015; 149: 1445–1450.
9. Slottosch I, Liakopoulos O, Kuhn E, et al. Lactate and lactate clearance as valuable tool to evaluate ECMO therapy in cardiogenic shock. *J Crit Care* 2017; 42: 35–41.
10. Tanaka D, Hirose H, Cavarocchi N, et al. The impact of vascular complications on survival of patients on venoarterial extracorporeal membrane oxygenation. *Ann Thorac Surg* 2016; 101: 1729–1734.
11. Avalli L, Sangalli F, Migliari M, et al. Early vascular complications after percutaneous cannulation for extracorporeal membrane oxygenation for cardiac assist. *Minerva Anestesiol* 2016; 82: 36–43.
12. Yang F, Hou D, Wang J, et al. Vascular complications in adult postcardiotomy cardiogenic shock patients receiving venoarterial extracorporeal membrane oxygenation. *Ann Intensive Care* 2018; 8: 72.
13. Pagani FD. Too much of a good thing? Reducing cannula size and flow rates during extracorporeal life support. *J Thorac Cardiovasc Surg* 2015; 149: 1434–1435.
14. Sakamoto S, Taniguchi N, Nakajima S, et al. Extracorporeal life support for cardiogenic shock or cardiac arrest due to acute coronary syndrome. *Ann Thorac Surg* 2012; 94: 1–7.
15. Takayama H, Landes E, Truby L, et al. Feasibility of smaller arterial cannulae in venoarterial extracorporeal membrane oxygenation. *J Thorac Cardiovasc Surg* 2015; 149: 1428–1433.

16. Kim J, Cho YH, Sung K, et al. Impact of cannula size on clinical outcomes in peripheral venoarterial extracorporeal membrane oxygenation. *ASAIO J* 2019; 65: 573–579.

17. Rupprecht L, Lunz D, Philipp A, et al. Pitfalls in percutaneous ECMO cannulation. *Heart Lung Vessel* 2015; 7: 320–326.

18. Lamelas J, Williams RF, Mawad M, et al. Complications associated with femoral cannulation during minimally invasive cardiac surgery. *Ann Thorac Surg* 2017; 103: 1927–1932.

19. Pozzi M, Henaine R, Grinberg D, et al. Total percutaneous femoral vessels cannulation for minimally invasive mitral valve surgery. *Ann Cardiothorac Surg* 2013; 2: 739–743.

20. Iserson KV. The origins of the gauge system for medical equipment. *J Emerg Med* 1987; 5: 45–48.

21. Kohler K, Valchanov K, Nias G, et al. ECMO cannula review. *Perfusion* 2013; 28: 114–124.

22. Montoya JP, Merz SI, Bartlett RH. A standardized system for describing flow/pressure relationships in vascular access devices. *ASAIO Trans* 1991; 37: 4–8.

23. Delius RE, Montoya JP, Merz SI, et al. New method for describing the performance of cardiac surgery cannulae. *Ann Thorac Surg* 1992; 53: 278–281.

24. Jones RT. Blood flow. *Ann Rev Fluid Mech* 1969; 1: 223–244.

25. Verdonck PR, Siller U, De Wachter DS, et al. Hydrodynamical comparison of aortic arch cannulae. *Int J Artif Organs* 1998; 21: 705–713.

26. De Wachter D, De Somer F, Verdonck P. Hemodynamic comparison of two different pediatric aortic cannulae. *Int J Artif Organs* 2002; 25: 867–874.

27. De Somer F. *Strategies for optimisation of paediatric cardiopulmonary bypass.* PhD Thesis, University of Groningen, Groningen, 2003.

28. Cheng N-S. Formula for the viscosity of a glycerol–water mixture. *Ind Eng Chem Res* 2008; 47: 3285–3288.

29. Rand PW, Lacombe E, Hunt HE, et al. Viscosity of normal human blood under normothermic and hypothermic conditions. *J Appl Physiol* 1964; 19: 117–122.

30. Riley JB, Zaidan JR. The immediate hemodynamic and metabolic effects of bolus injection of pharmacologic agents during cardiopulmonary bypass. *J Extra-Corpor Technol* 1983; 15: 71–77.

31. White FM. *Fluid mechanics.* 7th ed. New York: McGraw Hill, 2011.

32. Barnhart HX, Haber MJ, Lin LI. An overview on assessing agreement with continuous measurements. *J Biopharm Stat* 2007; 17: 529–569.

33. Koo TK, Li MY. A guideline of selecting and reporting intraclass correlation coefficients for reliability research. *J Chiropract Med* 2016; 15: 155–163.

34. Liu J, Tang W, Chen G, et al. Correlation and agreement: overview and clarification of competing concepts and measures. *Shanghai Arch Psychiatry* 2016; 28: 115–120.

35. Watson PF, Petrie A. Method agreement analysis: a review of correct methodology. *Theriogenology* 2010; 73: 1167–1179.

36. Wang S, Force M, Kunselman AR, et al. Hemodynamic evaluation of Avalon Elite bi-caval dual lumen cannulae and femoral arterial cannulae. *Artif Organs* 2019; 43: 41–53.

37. Qiu F, Lu CK, Palanzo D, et al. Hemodynamic evaluation of the Avalon Elite bi-caval dual lumen cannulae. *Artif Organs* 2011; 35: 1048–1051.

38. Wright G. Haemolysis during cardiopulmonary bypass: update. *Perfusion* 2001; 16: 345–351.

39. Kameneva MV, Burgreen GW, Kono K, et al. Effects of turbulent stresses upon mechanical hemolysis: experimental and computational analysis. *ASAIO J* 2004; 50: 418–423.

40. Vermeulen Windsant IC, de Wit NC, Sertorio JT, et al. Hemolysis during cardiac surgery is associated with increased intravascular nitric oxide consumption and perioperative kidney and intestinal tissue damage. *Front Physiol* 2014; 5: 340.

41. Vercaemst L. Hemolysis in cardiac surgery patients undergoing cardiopulmonary bypass: a review in search of a treatment algorithm. *J Extra Corpor Technol* 2008; 40: 257–267.

42. Mulholland JW, Massey W, Shelton JC. Investigation and quantification of the blood trauma caused by the combined dynamic forces experienced during cardiopulmonary bypass. *Perfusion* 2000; 15: 485–494.

43. Simons AP, Ganushchak YM, Teerenstra S, et al. Hypovolemia in extracorporeal life support can lead to arterial gaseous microemboli. *Artif Organs* 2013; 37: 276–282.

44. Ganushchak YM, Korver EP, Yamamoto Y, et al. Versatile minimized system—a step towards safe perfusion. *Perfusion* 2015; 31: 295–299.

45. Simons AP, Martens EG, Ganushchak YM, et al. Centrifugal pump performance during low-flow extracorporeal CO2 removal; safety considerations. *Perfusion* 2015; 30: 17–23.

46. Wang S, Chin BJ, Gentile F, et al. Potential danger of prepump clamping on negative pressure-associated gaseous microemboli generation during extracorporeal life support—an in vitro study. *Artif Organs* 2016; 40: 89–94.

47. Bachus L, Custodio A. *Know and understand centrifugal pumps.* Oxford: Elsevier, 2003.

48. Ganushchak Y, van Marken Lichtenbelt W, van der Nagel T, et al. Hydrodynamic performance and heat generation by centrifugal pumps. *Perfusion* 2006; 21: 373–379.

49. Budris AR. Centrifugal pump flow operating regions and impact on reliability, https://www.waterworld.com/articles/print/volume-32/issue-9/departments/pump-tips-techniques/centrifugal-pump-flow-operating-regions-and-impact-on-reliability.html (2016, accessed 23 November 2018).